Transmission and Trapping of Cold Electrons in Water Ice

Richard Balog, Peter Cicman, David Field,* Linda Feketeová,[†] and Kristin Hoydalsvik[‡]

Department of Physics and Astronomy, University of Aarhus, 8000 Aarhus C, Denmark

Nykola C. Jones

Institute for Storage Ring Facilities at Aarhus, University of Aarhus, 8000 Aarhus C, Denmark

Thomas A. Field

Department of Physics and Astronomy, Queen's University Belfast, Belfast, BT7 1NN, United Kingdom

Jean-Pierre Ziesel

Laboratoire Collisions Agrégats Réactivité-IRSAMC, Université Paul Sabatier and CNRS-UMR 5589, 31062 Toulouse Cedex, France

ABSTRACT: Experiments are reported which show that currents of low energy ("cold") electrons pass unattenuated through crystalline ice at 135 K for energies between zero and 650 meV, up to the maximum studied film thickness of 430 bilayers, indicating negligible apparent trapping. By contrast, both porous amorphous ice and compact crystalline ice at 40 K show efficient electron trapping. Ice at intermediate temperatures reveals metastable trapping that decays within a few hundred seconds at 110 K. Our results are the first to demonstrate full transmission of cold electrons in high temperature water ice and the phenomenon of temperature-dependent trapping.
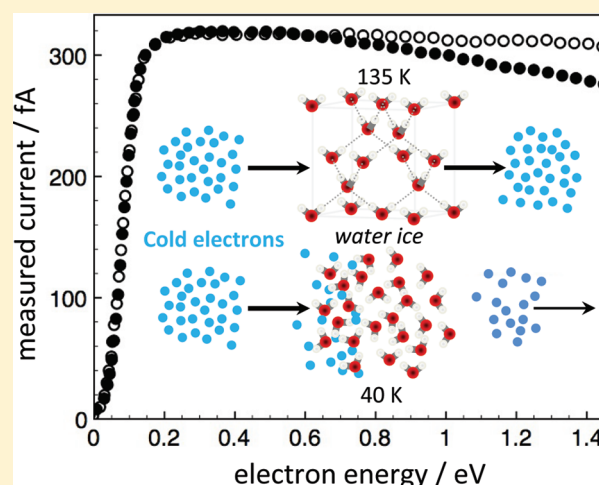
INTRODUCTION

A new phenomenon is reported here whereby ice shows strong temperature dependence for charging on bombardment by cold electrons. Ice in its natural state is subject to cold electron bombardment in the atmosphere of the Earth, for example in polar stratospheric clouds[1] and in the interstellar medium.[2] The interactions of electrons with ice also have implications in radiation chemistry and for techniques used for research into ice properties,[3] through ice charging and transmission characteristics. Here we find that ice at 135 K allows the full transmission of low energy electrons, suggesting that scanning tunnelling microscopy may be possible through thick layers of ice at this temperature.[4]

Electron beam studies of ice charging and transmission have to date involved only porous amorphous solid water (ASW) at temperatures below ∼30 K and used currents of >1 nA with an energy resolution of typically 100 meV.[5,6] Large capture cross sections have been found for low energy incident electrons.[7] For example, trapping cross sections of 0.5−1 Å^2 at energies of <1 eV have been reported for D_2O adsorbed on Pt(111) at 27 K.[8] The current state of knowledge is that low density porous ASW traps low energy electrons with a substantial cross-section. Here we describe new experiments carried out with an energy resolution >50 times higher than in any previous work and a total dose of electrons to the sample 2−3 orders of magnitudes lower. Damage to the ice is entirely negligible under the conditions of the present experiment.[9] We address the question whether high density nonporous ASW at higher temperatures around 100 K and also partially crystalline ice at 135 K traps electrons as readily as ice at 40 K. The answer is that we find strikingly different trapping characteristics for different temperatures.
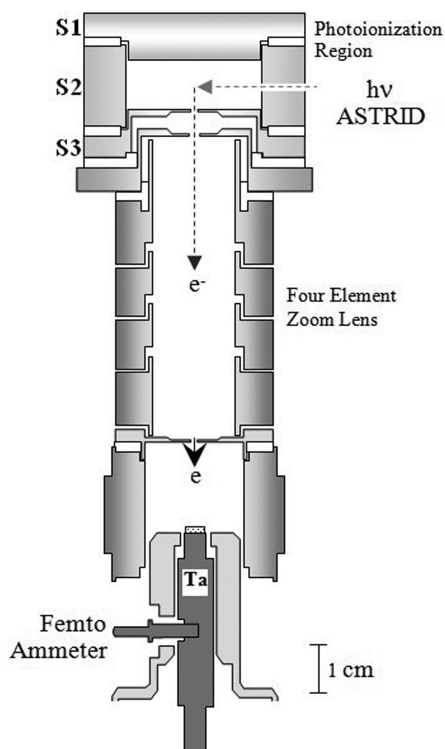
Figure 1. Scale diagram of the apparatus showing the electron photo-ionization source containing Ar using focused synchrotron radiation from the ASTRID storage ring at the Institute for Storage Ring Facilities in Aarhus (ISA). A four-element zoom lens guides the electron beam onto a sample adsorbed on tantalum or gold at energies between close to zero and up to 8 eV.

■ EXPERIMENTAL SECTION

In our experiment, a photoionization electron source is housed in an upper chamber and preparation of thin films of material on a tantalum or gold substrate is performed in a separate lower chamber, from which films are raised for subsequent irradiation. A schematic diagram of the UHV apparatus is shown in Figure 1 with the film in the raised position. Electrons are formed through threshold photoionization of high purity argon using synchrotron radiation from the undulator beamline on the ASTRID storage ring at Aarhus[10,11] tuning the wavelength of the radiation to a few meV above the ionization energy threshold for $^2P_{3/2}$ Ar^+ formation at 15.759 eV (78.676 nm). Photoelectrons have an energy resolution that is determined by the energy resolution in the photon beam, set here to ~1.6 meV full-width half-maximum. Electrons are formed into a beam and focused by a four-element electrostatic zoom lens. The apparatus is enclosed in a double μ-metal shield to exclude the magnetic field of the Earth or other stray fields. The background pressure is $\leq 10^{-10}$ mbar and the pressure in the apparatus with Ar present is ~10^{-7} mbar. Impurities in the Ar were found to introduce no detectable contamination over several hours exposure of substrates at 40 K.

Experiments used both Ta and Au substrates. The Ta substrate, which is cleaned by Ar ion sputtering and resistive heating to 750 K, is polycrystalline, with 60 μm cubic crystallites, and has a measured roughness which gives an effective surface area a few percent greater than the geometrical area. Auger spectroscopy shows that the Ta has a surface layer of TaC of thickness ~2.4 Å.

The Ta substrate was cooled with liquid nitrogen to a temperature of 135 $\pm$ 2 K. All experimental data at lower temperatures were obtained using a Au substrate and a helium cryo-cooler to obtain temperatures down to 40 K. Au is in the form of a 750 nm thick layer of polycrystalline material, grain size <100 nm, deposited on Ta. Au was cleaned by heating to 750 K.

Standard dosing techniques, using an effusive beam[12] or dosing from the background gas, allow the deposition of films of a known number of bilayers (BL), where 1 BL = 10^{15} molecules cm^{-2} and represents a single complete surface coverage for high density water ice. Techniques involve the use of a calibrated gas volume with absolute pressure drop measurements and the use of temperature programmed desorption (TPD) to obtain the conditions required to create a single monolayer. An ice layer separation of 0.32 nm was estimated from a density of 0.93 g cm^{-3}. The deposition rate of the ice in effusive beam dosing, used for submonolayer or very thin film preparation, was ~1 BL per 100 s and the angle of incidence of the incoming water molecules was <30°.[12,13] For background dosing, used for bulk ice experiments, the rate of deposition was ~1 BL per second. Errors in quoted film thicknesses are typically ±30%. Relative errors based on timing of the dose are a few percent. Values of film thickness were obtained by comparison with Xe, for which results were calibrated using temperature programmed desorption. Water was of grade CHROMASOLV Plus for HPLC (Sigma-Aldrich) and was degassed by repeated freeze−thaw cycles without further purification.

The current at the Ta or Au substrate is measured using a femto-ammeter (Keithley 6430). The energy of the electrons arriving at the target is given by the potential difference between their point of formation, at the center of the photoionization region, and the potential at the target surface-vacuum interface. The electron energy is varied by applying a variable offset potential to the entire electron source with respect to the sample. The zero of energy is taken to correspond to the value of offset potential for which current becomes accurately measurable, that is, 2−3 fA. The offset potential changes due to trapping of electrons on the surface or within the ice bulk by a measured value ΔV when the ice film is irradiated. ΔV is used to estimate charging cross sections.

■ RESULTS AND DISCUSSION

Figure 2 shows measurements of electron current versus energy where the upper curve is for porous ASW laid down at 40 K, showing no structure. The sample was warmed to 135 K to yield the middle curve, which shows clear structure, which is essentially preserved when the sample is cooled once more to 40 K (the lower curve). Structures, also seen on direct deposition at 135 K, are interpreted as diffraction features. These features cannot by themselves establish the form of ice present in the medium, save that it is crystalline, because the position of the conduction band and the energy dependent effective electron mass change both the absolute and relative values of the energy of diffraction features.[14] However, a very extensive literature (e.g. 4,15) shows that warming of ice from a few tens of K to 130−140 K results in the formation of a mixture of cubic and amorphous ice. Henceforth, we refer to ice laid down at 135 K as I_c ice.

To investigate charging, a first series of experiments was performed at 40 K, depositing submonolayer quantities of ice on an inert Xe spacer, thus effectively forming a parallel plate capacitor.[16,17] Analysis of the data proceeds as follows. If Σ_0 is a

6821

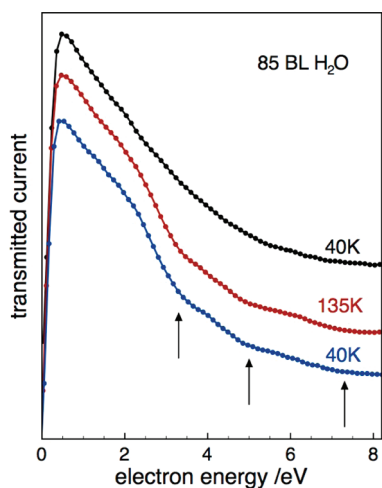dx.doi.org/10.1021/jp110475q |*J. Phys. Chem. A* 2011, 115, 6820–6824

Figure 2. Variation of the measured current for a 85 BL film of ice up to 8 eV. Top curve: porous ASW adsorbed at 40 K. Middle curve: the same sample warmed to 135 K. Lowest curve: the sample cooled once more to 40 K. The arrows mark the position of minima in the measured current arising from electron diffraction. Minima lie at 3.2, 5.0, and 7.5 eV. Curves are displaced for clarity. Maximum currents are 300 fA.

surface density equal to the number of available trap sites in a submonolayer, this quantity decreases exponentially in time according to $\Sigma = \Sigma_0 \exp(-\sigma J_0 t/e)$, where σ is the charge trapping cross-section, J_0 is the current incident for time t and e the electronic charge. The surface charge density P is given by $P = e(\Sigma - \Sigma_0) = e\Sigma_0[1 - \exp(-\sigma J_0 t/e)]$. Here we have very small total charge and the exponential may be expanded to first order without significant loss of accuracy yielding $P = \Sigma_0 \sigma J_0 t$. Because the system may be represented as a parallel plate capacitor, the capacitance of the system is given by $C = \varepsilon \varepsilon_0 A/L$, where ε is the relative permittivity of solid Xe, taken here to be 2, A is the effective area irradiated by our electron beam and L is the thickness of the Xe spacer layer. Since $C = Q/\Delta V$ it follows, using $J_0 t = Q/A$, that

$$\sigma = \frac{\varepsilon_0 \varepsilon \Delta V}{L \Sigma_0 J_0 t} \tag{1}$$

where ΔV, the change in the offset potential, was defined above.

Charging cross sections derived from experiments using 0.35 BL of ice on 150 monolayers of Xe are summarized in Table 1, using a current of 4.2 pA cm^{-2} and irradiating for 1200 s. Thus 0.35 BL on Xe at 40 K is found to charge strongly with energy dependent cross sections showing a maximum of 1.7 ± 0.85 Å^2 at 0.4 eV, similar to values reported in refs 5, 6 and 16 in which values are reported to rise to 3 Å^2 near to zero kinetic energy using an instrument with 0.1 eV resolution.

Turning to bulk ice, charge is accumulated within the film and the simple capacitor model described above is inappropriate. The relationship $P = e(\Sigma - \Sigma_0) = e\Sigma_0[1 - \exp(-\sigma J_0 t/e)]$ remains valid but we now introduce a model in which P decreases exponentially with distance toward the metal—ice interface, that is, that trapping is the dominant process. This yields

$$P = e\Sigma_0[1 - \exp(-\sigma J_0 t/e)]\exp(-\sigma n_0 l) \tag{2}$$

where Σ_0 has been replaced by n_0, a volume density, and l is the depth into the film. Given that the area irradiated is of much

Table 1. Summary of Data Showing the Characteristics of Experiments Performed with Films of Cubic/Amorphous Ice (labeled I_c), Submonolayer Ice, and Porous ASW. [a]

	electron energy/ eV	ice thickness/ BL	observed shift/mV	cross-section /Å^2
submonolayer ice at	0.1	0.35	5.5	0.95
40 K on 150 ML Xe	0.4		9	1.7
	1		3.5	0.7
	3		0.5–1	0.1
bulk I_c ice at 135 K	0.05–0.5	290	<1	<0.003
	0.08	430	<1	< 0.01
	0.4, 4, 8	430	<1	<0.006
porous ASW at 40 K	0.4	120	36.5	>1

[a] Cross sections for cubic/amorphous ice (I_c) at 135 K are net cross sections; see text.

greater dimension than l, the electric field in the film as a function of time and distance is given by

$$E(l,t) = \frac{1}{\varepsilon \varepsilon_0} e n_0 [1 - \exp(-\sigma J_0 t/e)] \int_0^l \exp(-\sigma n_0 l) dl$$
$$= \frac{e}{\sigma \varepsilon \varepsilon_0}[1 - \exp(-\sigma J_0 t/e)][1 - \exp(-\sigma n_0 l)] \tag{3}$$

The voltage difference $\Delta V(t)$ over the film is given by the integral of eq 3 over l for the range 0 to L and, hence

$$\Delta V(t) = \frac{e}{\sigma \varepsilon \varepsilon_0}[1 - \exp(-\sigma J_0 t/e)]\left\{ L - \frac{1}{\sigma n_0}[1 - \exp(\sigma n_0 L)]\right\} \tag{4}$$

The very low current allows eq 4 to be simplified to

$$\Delta V(t) = \frac{J_0 t}{\varepsilon \varepsilon_0}\left[L - \frac{1}{\sigma n_0}[1 - \exp(-\sigma n_0 L)]\right] \tag{5}$$

A second series of experiments was performed with bulk I_c ice at 135 K (with no spacer). The first entry for 135 K ice in Table 1 corresponds to a dose ($J_0 t$) of 12 pA cm^{-2} for 2530 s, the second to 2.2 pA cm^{-2} for 2000 s, and the third to 3.7 pA cm^{-2} for 2000 s. If the whole charge were trapped at the film—vacuum interface, effectively to form a capacitor, then experiments corresponding to the first entry, for example, would yield an observed shift of 22 mV, based on the capacitor model and using a relative permittivity $\varepsilon = 150$.[18] The observed shift lies below the detection limit of 1 mV. This suggests a very low trapping cross-section. The relevant process, as discussed below, is one in which electrons enter a trapping site with a high cross-section but, at 135 K, are released from any trapping site with a high probability. Thus, the net rate of trapping and the ambient concentration of trapped electrons is very small. The upper limits of cross sections for I_c ice at 135 K quoted in Table 1 and derived using eq 1 correspond therefore to net rates of trapping.

If by contrast high trapping cross sections are encountered, the second term within the square bracket in eq 5 is generally negligible. Equation 5 then reduces to the standard capacitor formula $\Delta V = QL/\varepsilon \varepsilon_0 A$, where Q/A, the charge/surface area, is $J_0 t$. Thus, ΔV becomes independent of σ for values above ~1−2 Å^2. This corresponds to the situation in bulk porous ASW at 40 K in which the whole charge is trapped very close to the

6822

dx.doi.org/10.1021/jp110475q |*J. Phys. Chem. A* 2011, 115, 6820–6824

vacuum−film interface. Hence, the quoted cross-section of 1 Å^2 is a lower limit, as shown. Uncertainties in the density of the ASW laid down at 40 K[13] lead to a maximum uncertainty of 25% for this lower limit. We remark in addition that films of I_c ice at 40 K, prepared by deposition of porous ASW at 40 K, warming to 135 K and then cooling to 40 K, also show substantial charging, with behavior similar to that of porous ASW at 40 K. In connection with the above discussion, note that the relative permittivity of ice at 40 K is ∼2, as opposed to ∼150 at 135 K.[18]

We have investigated intermediate temperatures by laying down ice and performing measurements at 105 and 110 K. In these cases, we observe voltage shifts, ΔV, of tens of mV as for ice deposited at 40 K. However, the voltage shift decays with a lifetime of a few hundred seconds. The abrupt change of behavior between 135, 110, and 40 K may be reproduced by a model in which electrons enter the ice, becoming trapped and then thermalized to the ice temperature through inelastic collisions, following which they may escape through tunnelling. The height and length of the barrier through which tunnelling takes place must be such that, at 135 K the trapping time, t_{trap}, is a few seconds, while at 110 K it is of the order of a few hundred seconds, and at 40 K effectively infinite on the experimental time scale. It may be shown[19] using a simple model of a one-dimensional square barrier that t_{trap} can be estimated from

$$t_{trap} = \frac{(m_e E_b)^{1/2} \pi z}{2\sqrt{2} E_{th}} sinh^2 \left[\frac{(2m_e E_b)^{1/2} d}{\hbar} \right] \qquad (6)$$

where m_e is the mass of the electron, E_b is the tunnelling barrier height, d its length, z the extension of the electron motion within the trap and E_{th} the thermal energy corresponding to the temperature of the ice. We assume that electrons have a frequency of between 10^{13} and 10^{14} Hz in a trap a few hundred K deep (a few tens of meV), corresponding to z of some tenths of 1 nm. We use 0.75 nm here which corresponds to a frequency of ∼2 × 10^{13} Hz, a figure appropriate to a very light but loosely bound particle. To satisfy the experimental constraints, the barrier length d is required to be ∼50 nm, giving t_{trap} = 3 s (135 K), 339 s (110 K), 3 years (40 K), and 1000 years (10 K). Electrons in the trap sites form polarons,[20] or solvated electrons in films, generated in our case through the oriented dipoles of the water molecules. The physical nature of traps and the dynamics of the electrons in ice have been discussed in detail in for example refs 21 and 22. The latter deals in particular with trapping at the surface of I_h ice at ≥150 K, showing substantial structural change and reorganization of water molecules around an excess electron. Similar rearrangement may give rise to long-lived surface trap states in liquid water.[23] There appear to be no detailed studies on structural rearrangement associated with excess electrons in cubic ice, of relevance here for lower temperatures. There is however clear indication that subsurface rearrangement is likely to be strongly hindered in colder ice.[22] This is consistent with our conclusion that electrons are trapped at or very close to the ice/vacuum interface.

We turn now to the transmission properties of I_c ice at 135 K, at which temperature as we have seen there is no effective charging. In Figure 3 we show two representative low energy scans for 12 and 430 BL. Data in Figure 3 show that the measured current is unaffected by the presence of the ice film at all energies up to 650 meV. The ratio of measured currents for different films is found to have the same value of unity up to 650 meV for all films studied. This is observed for both Ta and Au substrates.
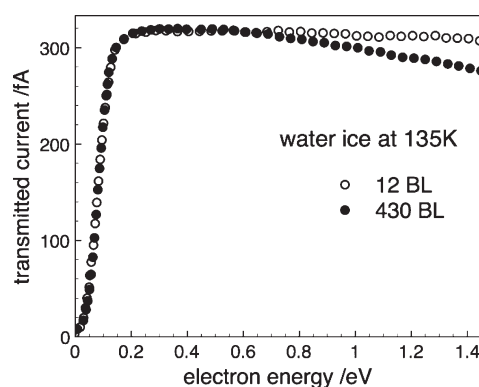

Figure 3. Variation with incident electron energy of the measured current through a 12 BL and a 430 BL film of ice between a few meV and 1.4 eV for I_c ice laid down and held at 135 K.

These data confirm that we probe properties of the bulk of the ice and not of the ice−metal interface.

Independence of transmission on film thickness in 135 K I_c ice requires that once the electron has entered the film, the transmission is unity. We propose that this effective transparency of the film arises through the thermalization of electrons in defects, through inelastic interactions involving both phonons and local modes,[5,24,25] which are considerably enhanced through the transient trapping described earlier. These events lead to irreversible thermalization into states below the vacuum level from which electrons can no longer return to the vacuum,[26,27] given a conduction band which straddles the vacuum level.[28] All electrons therefore pursue a path through the ice film which must lead to their passage into the metal substrate. The observed thickness independent transmission at very low energy for 135 K ice is an indication that thermalization occurs very close to the film−vacuum interface, thus showing an efficient interaction of electrons with trapping sites, consistent with our earlier discussion.

Data in Figure 4 show how transmission of 135 K I_c ice decreases with increasing film thickness at energies >650 meV up to energies of 8 eV. These data suggest that electrons at energies >650 meV can escape from the film. This escape takes place with increasing probability as energy rises since an increasing proportion will remain above the vacuum level despite inelastic scattering. The greater drop in transmission for thicker films arises through multiple elastic and inelastic scattering within the film, an effect that evidently saturates with thick films. Note that the diffraction pattern, seen both in Figure 2 and Figure 4, reflects the variation of the density of states with energy in the conduction band above the vacuum level. Further, porous ASW shows similar scattering behavior at higher energies. In this connection, the mean free path in porous ASW has been reported as ∼3 nm, or ∼10 BL, in the energy range between 1.7 and 9 eV.[5]

■ CONCLUDING REMARKS

In conclusion, these very first experiments in which high resolution electron beams have been allowed to impinge at very low energy on ice have revealed that ice shows charging characteristics which are strongly temperature dependent. I_c ice at 135 K retains electrons briefly in a metastable trapped state for a few seconds whereas at lower temperatures trapping times may extends to many years or longer. The tunneling model proposed to explain these results is primitive, but indicates that there exist
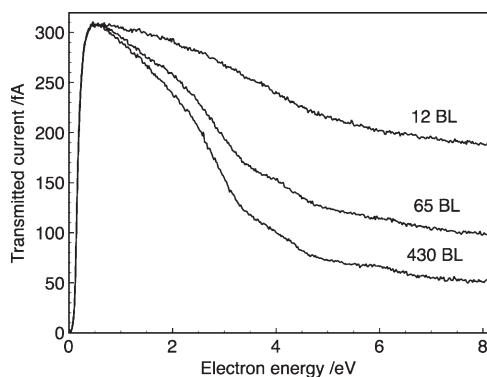
Figure 4. Variation with incident electron energy of the measured current through a 12, 65 and 430 BL film of ice up to 8 eV for I_h ice laid down at 135 K.

very long shallow barriers through which electrons penetrate efficiently when thermalized at 135 K but with a very low rate when thermalized at 40 K.

Our data are relevant to an understanding of dense interstellar clouds where ~20 eV electrons are formed by cosmic ray ionization of H_2. In a typical cloud of density 10^4 cm^{-3} and temperature 10−20 K, electrons cool within a year to the local temperature. Cold electrons typically encounter grains, coated with the majority species amorphous water ice of tens of BL in thickness, a net 50−100 times within a cloud lifetime of 10^7 years. Thus, a population of electrons with E_{th} = 10 K, mobile on a 1000 year time scale, will become trapped in the ice. Our data show that these electrons are unable to escape to vacuum and will therefore tunnel within the mantle, with the possibility of initiating reactions involving minority species embedded within the ice. For example, the formation of glycine, identified in meteorites, through reactions of NH_3 or hydroxylamine (NH_2OH) with CH_3COOH and amino-alcohols with $HCOOH$ could be initiated by electrons trapped within grain mantles[29] through negative ion formation. Further, as a protostar forms in such a cold dense cloud, the grain mantles will begin to warm and the electron mobility will increase and enhance electron-induced chemistry within the mantle, contributing to the gas phase molecular complexity that is associated with warm cores.[30]

■ AUTHOR INFORMATION

Corresponding Author
*E-mail: dfield@phys.au.dk.

Present Addresses
†ARC Centre of Excellence for Free Radical Chemistry and Biotechnology, Bio21 Institute of Molecular Science and Biotechnology, School of Chemistry, The University of Melbourne, Victoria 3010, Australia.
‡Norwegian University of Science and Technology, Department of Physics Høgskoleringen 5, Trondheim, Norway.

We would like to thank Dr. J. Wells (Aarhus) for carrying out investigations of the tantalum surface.

■ REFERENCES

(1) Lu, Q.-B.; Sanche, L. *Phys. Rev. Lett.* **2001**, *87*, 078501.
(2) Field, D.; Balog, R.; Feketeova, L.; Jones, N.C.; et al. In *Molecules and Space and Laboratory*; Lemaire, J. L., Combes, F., Eds.; S. Diana: Paris, 2007.
(3) Henderson, M. A. *Surf. Sci. Rep* **2002**, *46*, 1.
(4) Thurmer, K.; Bartelt, N. C. *Phys. Rev. B* **2008**, *77*, 0195425.
(5) Michaud, M.; Wen, A.; Sanche, L. *Radiat. Res.* **2003**, *159*, 3.
(6) Simpson, W. C.; Orlando, T. M.; Parenteau, L.; Nagesha, K.; Sanche, L. *J. Chem. Phys.* **1998**, *108*, 5027.
(7) Bass, A. D.; Sanche, L. *J. Chem. Phys.* **1991**, *95*, 2910.
(8) Simpson, W. C.; Orlando, T. M.; Parenteau, L.; Nagesha, K.; Sanche, L. *J. Chem. Phys.* **1998**, *108*, 5027.
(9) Mehlhorn, M.; Gawronmski, H.; Morgernstern, K. *Phys. Rev. Lett.* **2008**, *101*, 0196101.
(10) Hoffmann, S. V.; Lunt, S. L.; Jones, N. C.; Field, D.; Ziesel, J. P. *Rev. Sci. Instrum.* **2002**, *73*, 4157.
(11) Curik, R.; Ziesel, J. P.; Jones, N. C.; Field, T. A.; Field, D. *Phys. Rev. Lett.* **2006**, *97*, 123202.
(12) Buckman, J.; Gulley, R. J.; Moghbelalhossien, M.; Bennett, S. J. *Meas. Sci. Technol.* **1993**, *4*, 1143.
(13) Stevenson, K. P.; Kimmel, G. A.; Dohnalek, Z.; Smith, R. S.; Kay, B. D. *Science* **1999**, *283*, 1505.
(14) Bader, G.; Perluzzo, G.; Caron, L. G.; Sanche, L. *Phys. Rev. B* **1984**, *30*, 78.
(15) Petrenko, V. F.; Whitworth, R. W. *Physics of Ice*; Oxford University Press: London, 1999.
(16) Naaman, R.; Sanche, L. *Chem. Rev.* **2007**, *107*, 1553.
(17) Marsolais, R. M.; Deschênes, M.; Sanche, L. *Rev. Sci. Instrum.* **1989**, *60*, 2724.
(18) Tsekouras, A. A.; Iedema, M. J.; Cowin, J. P. *Phys. Rev. Lett.* **1998**, *80*, 5798.
(19) Field, D. *Astron. Astrophys.* **2000**, *362*, 774.
(20) Ge, N.-H.; Wong, C. M.; Lingle, R. L.; McNeill, D. J. D.; Gaffney, K. J.; Harris, C. B. *Science* **1998**, *297*, 202.
(21) Gahl, C.; Bovensiepen, U.; Frischkorn, C.; Wolf, M. *Phys. Rev. Lett.* **2002**, *89*, 0107402.
(22) Baletto, F.; Cavazzoni, C.; Scandolo, S. *Phys. Rev. Lett.* **2005**, *95*, 176801.
(23) Skorobogatiy, M.; Park, I. J.; Joannopoulos., J. D. *Comput. Mater. Sci.* **2005**, *32*, 96.
(24) Li, J. *J. Chem. Phys.* **1996**, *105*, 6733.
(25) Kolenikov, A. I.; Li, J.; Parker, S. F.; Eccleston, R. S.; Loong, C.-K. *Phys. Rev. B* **1999**, *59*, 3569.
(26) Steinberger, I. T.; Bass, A. D.; Schechter, R.; Sanche, L. *Phys. Rev. B* **1993**, *48*, 8290.
(27) Fano, U.; Stephens, J. A. *Phys. Rev. B* **1986**, *34*, 438.
(28) Grand, D; Bernas, A. *Chem. Phys. Lett.* **1983**, *97*, 119.
(29) Lafosse, A.; Bertin, M.; Domaracka, A.; Pliska, D.; Illenberger, E.; Azria, R. *Phys. Chem. Chem. Phys.* **2006**, *8*, 5564.
(30) Awad, Z.; Viti, S.; Collings, M. P; Williams, D. A. *Mon. Not. R. Astron. Soc.* **2010**, *407*, 2511.